Search for a new gauge boson in π^0 decays

J. Altegoer, P. Astier, D. Autiero, A. Baldisseri, M. Baldo-Ceolin, G. Ballocchi, M. Banner, S. Basa, G. Bassompierre, K. Benslama, et al.

EUROPEAN ORGANIZATION FOR NUCLEAR RESEARCH

CERN-EP/98-047
23 March 1998

SEARCH FOR A NEW GAUGE BOSON IN π^0 DECAYS

The NOMAD Collaboration

Abstract

A search was made for a new light gauge boson X which might be produced in $\pi^0 \to \gamma + X$ decay from neutral pions generated by 450-GeV protons in the CERN SPS neutrino target. The X's would penetrate the downstream shielding and be observed in the NOMAD detector via the Primakoff effect, in the process of $X \to \pi^0$ conversion in the external Coulomb field of a nucleus. With 1.45×10^{18} protons on target, 20 candidate events with energy between 8 and 140 GeV were found from the analysis of neutrino data. This number is in agreement with the expectation of 18.1 ± 2.8 background events from standard neutrino processes. A new 90 % *C.L.* upper limit on the branching ratio $Br(\pi^0 \to \gamma + X) < (3.3 \text{ to } 1.9) \times 10^{-5}$ for X masses ranging from 0 to 120 MeV/c^2 is obtained.

Submitted to Physics Letters B

The NOMAD Collaboration

J. Altegoer[6] P. Astier[15] D. Autiero[9] A. Baldisseri[19] M. Baldo-Ceolin[14] G. Ballocchi[9] M. Banner[15] S. Basa[10] G. Bassompierre[2] K. Benslama[10] N. Besson[19] I. Bird[10,9] B. Blumenfeld[3] F. Bobisut[14] J. Bouchez[19] S. Boyd[20] A. Bueno[4] S. Bunyatov[7] L. Camilleri[9] A. Cardini[11] A. Castera[15] P.W. Cattaneo[16] V. Cavasinni[17] A. Cervera-Villanueva[9] G.M. Collazuol[14] G. Conforto[22] C. Conta[16] M. Contalbrigo[14] R. Cousins[11] D. Daniels[4] A. De Santo[17] T. Del Prete[17] T. Dignan[4] L. Di Lella[9] E. do Couto e Silva[9] I.J. Donnelly[20,21] J. Dumarchez[15] T. Fazio[2] G.J. Feldman[4] R. Ferrari[16] D. Ferrère[9] V. Flaminio[17] M. Fraternali[16] J-M. Gaillard[2] P. Galumian[10] E. Gangler[15] A. Geiser[9] D. Geppert[6] D. Gibin[14] S.N. Gninenko[13] J-J. Gomez-Cadenas[1,9] J. Gosset[19] C. Gößling[6] M. Gouanère[2] A. Grant[9] G. Graziani[8] A. Guglielmi[14] C. Hagner[19] J. Hernando[1,25] D. Hubbard[4] P. Hurst[4] N. Hyett[12] E. Iacopini[8] C. Joseph[10] D. Kekez[23] B. Khomenko[9] M.M. Kirsanov[13] O. Klimov[7] J. Kokkonen[9] A.V. Kovzelev[13] V. Kuznetsov[7] S. Lacaprara[14] A. Lanza[16] L. La Rotonda[5] M. Laveder[14] A. Letessier-Selvon[15] J-M. Levy[15] L. Linssen[9] A. Ljubičić[23] J. Long[3,26] A. Lupi[8] E. Manola-Poggioli[2,9] A. Marchionni[8] F. Martelli[22] X. Méchain[19] J-P. Mendiburu[2] J-P. Meyer[19] M. Mezzetto[14] S.R. Mishra[4] G.F. Moorhead[12] L. Mossuz[2] P. Nédélec[2,9] Yu. Nefedov[7] C. Nguyen-Mau[10] D. Orestano[18] F. Pastore[18] L.S. Peak[20] E. Pennacchio[22] J-P. Perroud[10] H. Pessard[2] R. Petti[16] A. Placci[9] H. Plothow-Besch[9] A. Pluquet[19] G. Polesello[16] D. Pollmann[6] B.G. Pope[9] B. Popov[7,15] C. Poulsen[12] P. Rathouit[19] C. Roda[9,17] A. Rubbia[9] F. Salvatore[16] D. Scannicchio[16] K. Schahmaneche[15] B. Schmidt[6] A. Sconza[14] M. Serrano[15] M.E. Sevior[12] D. Sillou[2] F.J.P. Soler[20] G. Sozzi[10] D. Steele[3,10] P. Steffen[9] M. Steininger[10] U. Stiegler[9] M. Stipčević [23] T. Stolarczyk[19] M. Tareb-Reyes[2,10] G.N. Taylor[12] S. Tereshchenko[7] A.N. Toropin[13] A-M. Touchard[15] S.N. Tovey[12] M-T. Tran[10] E. Tsesmelis[9] J. Ulrichs[20] V. Uros[15] M. Valdata-Nappi[5,24] V. Valuev[7,2] F. Vannucci[15] K.E. Varvell[20,21] M. Veltri[22] V. Vercesi[16] D. Verkindt[2] J-M. Vieira[10] T. Vinogradova[11] M-K. Vo[19] S.A. Volkov[13] F. Weber[4] T. Weisse[6] M. Werlen[10] F. Wilson[9] L.J. Winton[12] B.D. Yabsley[20] H. Zaccone[19] K. Zuber[6]

[1]Univ. of Massachusetts, Amherst, MA, USA
[2]LAPP, Annecy, France
[3]Johns Hopkins Univ., Baltimore, MD, USA
[4]Harvard Univ., Cambridge, MA, USA
[5]Univ. of Calabria and INFN, Cosenza, Italy
[6]Dortmund Univ., Dortmund, Germany
[7]JINR, Dubna, Russia
[8]Univ. of Florence and INFN, Florence, Italy
[9]CERN, Geneva, Switzerland
[10]University of Lausanne, Lausanne, Switzerland
[11]UCLA, Los Angeles, CA, USA
[12]University of Melbourne, Melbourne, Australia
[13]Inst. Nucl. Research, INR Moscow, Russia
[14]Univ. of Padova and INFN, Padova, Italy
[15]LPNHE, Univ. of Paris, Paris VI and VII, France
[16]Univ. of Pavia and INFN, Pavia, Italy
[17]Univ. of Pisa and INFN, Pisa, Italy
[18]Roma-III Univ., Rome, Italy
[19]DAPNIA, CEA Saclay, France
[20]Univ. of Sydney, Sydney, Australia
[21]ANSTO,Sydney, Menai, Australia
[22]Univ. of Urbino, Urbino, and INFN Florence, Italy
[23]Rudjer Bošković Institute, Zagreb, Croatia
[24]Now at Perugia Univ., Perugia, Italy
[25]Now at UCSC, Santa Cruz, CA, USA
[26]Now at Univ. of Colorado, Boulder, CO, USA

1 Introduction

Many extensions of the Standard Model such as GUTs [1], super-symmetric [2], super-string models [3] and models including a new long-range interaction, i.e. the fifth force [4], predict an extra $U^{'}(1)$ factor and therefore the existence of a new gauge boson X corresponding to this new group. The predictions for the mass of the X boson are not very firm and it could be light enough ($M_X \ll M_Z$) for searches at low energies.

If the mass M_X is of the order of the pion mass, an effective search could be conducted for this new vector boson in the radiative decays of neutral pseudoscalar mesons $P \to \gamma + X$, where $P = \pi^0, \eta$, or η', because the decay rate of $P \to \gamma$ + *any new particles with spin 0 or* $\frac{1}{2}$ proves to be negligibly small [5]. Therefore, a positive result in the direct search for these decay modes could be interpreted unambiguously as the discovery of a new light spin 1 particle, in contrast with other experiments searching for light weakly interacting particles in rare K, π or μ decays [5, 6].

From the analysis of the data from earlier experiments, constraints on the branching ratio for the decay of $P \to \gamma + X$ range from 10^{-7} to 10^{-3} depending on whether X interacts with both quarks and leptons or only with quarks. Since in the first case X is a short lived particle decaying mainly to e^+e^- or $\nu\overline{\nu}$ pairs, we will only consider the second case, where X is a relatively long-lived particle [6].

Direct searches for a signal from $\pi^0 \to \gamma + X$ decay have been performed in a few experiments with two different methods: i) searching for a peak in inclusive photon spectra from two-body $\pi^0 \to \gamma + nothing$ decays, where "nothing" means that X is not detected because it either has a long life time or decays into $\nu\overline{\nu}$ pairs (ref. [7, 8, 9]); and ii) searching for a peak in the invariant mass spectrum of e^+e^- pairs from π^0 decays, which corresponds to the decay $X \to e^+e^-$ [10].

The best experimental limit on the decay $\pi^0 \to \gamma + X$ was obtained recently by the Crystal Barrel Collaboration at CERN [9]. Using $p\overline{p}$ annihilations as a source of neutral pions, they searched for a single peak in the inclusive photon energy spectrum. The branching ratio limit of (6 to 3)$\times 10^{-5}$ (90%$C.L.$) was obtained for $65 < M_X < 125\ MeV$. A less stringent upper limit $BR(\pi^0 \to \gamma + X) <$ (3 to 0.6)$\times 10^{-4}$ was obtained for the mass region $0 < M_X < 65\ MeV/c^2$. This result is valid for the case where X is a long-lived particle or it decays mainly to $\nu\overline{\nu}$ pairs.

In this paper, we present a more sensitive upper limit on the branching ratio of the decay $\pi^0 \to \gamma + X$ obtained by using a new method [11] from the analysis of high energy neutrino data taken by the NOMAD experiment at CERN.

2 The NOMAD Detector

The NOMAD detector, designed to search for a neutrino oscillation signal in the CERN SPS wide-band neutrino beam, is described in detail in ref.[12]. A sketch of the NOMAD detector is shown in Figure 1. It consists of a number of subdetectors most of which are located inside a 0.4 T dipole magnet with a volume of 7.5×3.5×3.5 m^3. The relevant features for the present study will be briefly mentioned.

The complete active target consists of 44 drift chambers (DC) mounted in 11 modules [13]. The target is followed by a transition radiation detector (TRD) to enhance e/π separation and by a lead-glass electromagnetic calorimeter (ECAL) with an upstream preshower detector (PRS). Five additional drift chambers are installed in the TRD region.

Each of the 9 TRD modules [14] consists of a radiator followed by a detection plane of vertical straw tubes.

The ECAL consists of 875 lead-glass Cerenkov counters of TF1-000 type arranged in a matrix of 35 rows by 25 columns. Each counter is about 19 radiation lengths deep. The energy resolution

is $\sigma/E = 0.01 + 0.032/\sqrt{E}$, where E is the shower energy in GeV. A more detailed description of the ECAL is given elsewhere [15].

The PRS is composed of two planes of proportional tubes (286 horizontal and 288 vertical tubes) preceded by a 9 mm thick (1.6 X_0) lead plate, providing a spatial resolution $\sigma_{x,y} \approx 1cm/\sqrt{E}$, where E is the shower energy in GeV. The fiducial mass of this detector is about 700 kg.

The trigger for neutrino interactions in the target is provided by two planes of scintillation counters T_1 and T_2. A veto in front of the magnet rejects upstream neutrino interactions and muons incident on the detector. Neutrino interactions in the PRS or ECAL are collected by a $\overline{T_1 \times T_2} \times ECAL$ trigger specially designed for this purpose. The ECAL signal is obtained as the OR of all counter signals exceeding a threshold of about 0.8 GeV. The timing of this signal depends on the deposited energy. For energies above 3 GeV a time resolution of a few ns and a trigger efficiency of 100% are obtained. The average rate of the $\overline{T_1 \times T_2} \times ECAL$ trigger is about 3/ 10^{13} protons on the neutrino target (p.o.t.).

A hadronic calorimeter(HCAL) and a set of 10 drift chambers placed behind the magnet provide an estimate of the energy of the hadronic component in the event and muon identification, respectively. The HCAL is an iron-scintillator sampling calorimeter consisting of 11 iron plates, 4.9 cm thick, separated by 1.8 cm gaps in which scintillator paddles 3.6 m long 1 cm thick, and 18.3 cm wide are installed. The HCAL active area is 3.6 m wide by 3.5 m high, and approximately 3.1 hadronic interaction lengths deep.

3 Method of Search

If the decay $\pi^0 \to \gamma + X$ exists, one expects a flux of high energy X bosons from the SPS neutrino target, since π^0's are abundantly produced in the forward direction by 450 GeV protons either in the beryllium target or in the beam dump following the decay tunnel. If X is a long-lived particle, this flux would penetrate the downstream shielding without significant attenuation and would be observed in the NOMAD detector via the Primakoff effect, namely in the conversion process $X \to \pi^0$ in the external Coulomb field of a nucleus [11] (see Figure 2).

Because the cross section for $X \to \pi^0$ conversion is proportional to Z^2, we searched for these events in the lead of the preshower detector. The experimental signature of $X \to \pi^0$ conversion is a single high energy π^0 decaying into two photons which results in a single isolated electromagnetic shower in the ECAL. The corresponding ECAL cluster should be matched to the PRS cluster from the converted photons and must not be accompanied by a significant activity in any of the other NOMAD subdetectors. The occurrence of $X \to \pi^0$ conversion would appear as an excess of neutrino-like interactions in the PRS with pure electromagnetic final states above those expected from Monte Carlo predictions of standard neutrino interactions.

The expected energy spectrum of X-bosons at the NOMAD detector is shown in Figure 3 for a mass M_X=10 MeV. The energy spectra of π^0's produced in the neutrino target and in the beam dump have been obtained with the same detailed GEANT [16] simulation used to predict the neutrino flux distributions at the NOMAD detector. The X-spectrum is considerably harder than that of neutrinos which is also shown for comparison.

4 Data Sample and Event Selection

This analysis is based on the data taken during the first half of the neutrino run in 1995, in which the NOMAD target was only partially installed and consisted of four drift chamber modules placed upstream of the TRD detector. The integrated number of protons delivered to the neutrino target during this period was about 1.45 $\times 10^{18}$.

Monte Carlo simulations use the LEPTO 6.1 event generator [17] supplemented by event generators for resonance, quasi-elastic and coherent neutrino processes and a full detector simulation based on GEANT[16]. These simulations together with direct measurements of subdetector occupancy during the neutrino spill with a random trigger [12] show that ν and $X \to \pi^0$ events in the PRS are accompanied by no significant activity in the DC and TRD. For this reason a simple cut on the number of hits N_{hit}^{DC}, $N_{hit}^{DC(TRD)}$ and N_{hit}^{TRD} in the DC, in the DC located in the TRD region, and in the TRD, respectively, were used as a veto to suppress events from neutrino interactions which occurred in these regions or in the magnet coils. However, neutrino events, mainly with a neutral final state, which occurred in the near upstream PRS region can also pass these veto cuts and can be taken as neutrino events in the PRS. For this reason the upstream region was also included in the simulations and surviving events were considered as neutrino events in the PRS.

The selection criteria for $X \to \pi^0$ events are based on a full Monte Carlo simulation of $X \to \pi^0$ conversions in the NOMAD detector and rely on their properties as mentioned in Section 3, namely:

- the quality of the match between the ECAL shower and the corresponding PRS cluster;
- the total energy and the shower shape in the ECAL;
- the amount of energy deposition in the HCAL.

Candidate events were identified by the following simultaneous requirements:

- $\overline{DC} \times \overline{TRD}$ (no activity in the DC or TRD): $N_{hit}^{DC} \leq 10$, $N_{hit}^{DC(TRD)} \leq 4$, $N_{hit}^{TRD} \leq 2$.

- $PRS \times ECAL(> 8\ GeV)$: isolated PRS cluster matched to isolated ECAL cluster in both X and Y planes.

  At most two ECAL clusters in the ECAL were allowed. The energy of the most energetic cluster had to be $E_{ECAL} > 8\ GeV$ and the second cluster had to be less than 0.3 GeV in order to reject pile-up events and ECAL noise. The shape of the most energetic cluster was fitted to the shape expected from an electromagnetic shower and the χ^2 of the fit was required to be less than 20 [18]. The differences ΔX and ΔY between the X and Y coordinates of the cluster in the PRS and the corresponding cluster in the ECAL were required to be $|\Delta X| < 2\ cm$, $|\Delta Y| < 1.5\ cm$.

  These conditions were used to identify isolated electromagnetic showers in the ECAL that originated from the conversion of photons from π^0's produced in the preshower.

- $\overline{HCAL}$ (no HCAL activity): the total visible energy was required to be less than the HCAL noise threshold $E_{HCAL} < 0.4\ GeV$.

  This cut serves to identify electromagnetic energy in the ECAL. The reliability of the HCAL veto to suppress conventional neutrino events with an energy leakage to the HCAL detector was checked with straight through muons and with a selected sample of ν_μ charged current (CC) events in the PRS.

- $\overline{MUON}$: no track(s) in the muon chambers matched to the PRS cluster.

After applying these cuts to the initial sample of 4.83×10^5 events recorded with the ECAL trigger we found 20 candidate events for $X \to \pi^0$ conversion. The amount of background in this sample from standard ν_μ and ν_e interactions was evaluated using the Monte Carlo (see Section 5).

Applying the $\overline{DC} \times \overline{TRD} \times PRS \times ECAL(> 1GeV) \times MUON$ selection criteria to the same initial sample we find 3691 events from $\nu_\mu CC$ interactions in the PRS. Here, $MUON$ denotes single muon tracks extrapolated back from the muon chambers to the PRS and matched to the PRS cluster. The spectra of energy deposited in the ECAL for these selected $\nu_\mu CC$ events and for simulated events which pass the same reconstruction program and selection cuts are found to be in agreement. The $\overline{T_1 \times T_2} \times ECAL$ trigger efficiency was obtained from a Monte Carlo simulation and was found to be 71% and 97% for $\nu_\mu CC$ and $X \to \pi^0$ events, respectively. Taking the overall selection efficiency into account, the total number of $\nu_\mu CC$ events interacting in the PRS was found to be $N_{\nu_\mu CC}$=2.29×10^4. The number of $\nu_\mu CC$ events was converted to the number of protons on target N_{pot} using the simulation of the neutrino flux at the NOMAD detector and the known cross section value for $\nu_\mu CC$ interactions, giving $N_{pot} = 1.36 \times 10^{18}$. This number agrees within 10% with the value of N_{pot} measured by the beam monitors and was used further for normalisation. The main uncertainty results from the contribution of events from neutrino interactions in the downstream TRD region which pass the DC and TRD cuts and from backscattering in events occurring in the PRS. By varying the $\overline{DC}$ and $\overline{TRD}$ cuts, it was found that the systematic error in the number of $\nu_\mu CC$ events in the PRS resulting from backscattering is of the order of 10%.

5 Background Events

The main background to $X \to \pi^0$ conversions is expected from the following neutrino processes occurring in the PRS or upstream PRS region with a significant electromagnetic component in the final state and with no significant energy deposition in the HCAL :

- $\nu_\mu CC$ interactions classified as muonless because the muon was not detected;
- inclusive π^0 production from ν_μ neutral current (NC) interactions;
- coherent and diffractive π^0 production;
- quasi-elastic ν_e scattering.
- $\nu_e CC$ interactions;

Backgrounds from the trident events, $\nu_e + Pb \to \nu_e + e^+ + e^- + Pb$ and from pile-up events were found to be negligible.

To evaluate the amount of background in the data sample, simulated events were processed through the same reconstruction program and selection criteria that were used for real neutrino data. Then, all background distributions were summed up, taking into account the corresponding normalisation factors. These factors were calculated from beam composition and cross sections of the well-known processes listed above. The total number of events interacting in the PRS and the number of expected candidate events after applying the selection criteria are given in Table 1 for each background process.

The total background in the data sample was estimated to be 18.1±2.8 events, where statistical and systematic errors are added in quadrature. The fraction of neutrino interactions in the PRS which satisfy all cuts is 6×10^{-4}.

6 Result

Figure 4 shows the combined background and candidate event energy spectra in the ECAL. The agreement between data and Monte Carlo is good. The overall efficiency for $X \to \pi^0$ conversion

Table 1: Overall background estimate

item	$\nu_\mu CC$	$\nu_\mu NC$	Coh.π^0	$\nu_e - QE$	$\nu_e CC$
Total number of interactions in the PRS	22886	6866	59	6.2	320
Number of expected candidate events	1.7±1.0	6.6±1.3	1.5±0.4	2.1±0.2	6.2±1.2

detection was found to be ≈24%. The inefficiency is mostly due to the requirement that at least one photon from π^0 decay convert in the PRS.

By subtracting the number of expected background events from the number of candidate events we obtain $N_{X\to\pi^0} = 1.9\pm5.3$ events showing no excess of $X \to \pi^0$ conversion-like events, and, hence, no indication for the existence of this process. The 90% *C.L.* upper limit for the branching ratio $Br(\pi^0 \to \gamma + X)$ was calculated by using the following relation:

$$N^{90\%}_{X\to\pi^0} > [Br(\pi^0 \to \gamma + X)]^2 \times \int \frac{df_0(M_X, E_X, N_{pot})}{dE_X}\sigma_0(M_X, E_X)dE_X \times \varepsilon_{sel} \times \rho l \frac{N_A}{A} \qquad (1)$$

where $N^{90\%}_{X-\pi^0}$ (= 8.7 events) is the 90% *C.L.* upper limit for the expected number of signal events, ε_{sel} is the selection efficiency, which was found to be practically independent of E_X, $f_0(M_X, E_X, N_{pot})$ and $\sigma_0(M_X, E_X)$ are the flux of X bosons for the given number of protons N_{pot} on the neutrino target and the cross section for $X \to \pi^0$ conversion on lead, respectively, calculated for $Br(\pi^0 \to \gamma + X)$=1. In Eq.(1), M_X and E_X are the mass and energy of the X boson, respectively. The cross section $\sigma_0(M_X, E_X)$ is given in ref. [11]. The total $X-$flux per proton on target calculated as a function of the X boson mass is shown in Figure 5. We note that $Br(\pi^0 \to \gamma + X)$ appears twice in the formula for $N_{X\to\pi^0}$, through the X boson flux from the target and through the Primakoff mechanism.

The 90 % *C.L.* branching ratio limit curve is shown in Figure 6 together with the result of ref. [9]. For the mass region 0< M_X < 120 MeV/c^2 the limit is

$$Br(\pi^0 \to \gamma + X) < (3.3\ to\ 1.9) \times 10^{-5} \qquad (2)$$

Varying the cut on the ECAL energy deposition in the range from 5 to 50 GeV does not change the limit substantially, while above 50 GeV it becomes worse. The limit is valid for an X boson lifetime $\tau_X > 10^{-9} M_X[MeV/c^2]$ s. For the mass region 0< M_X < 60 MeV/c^2, the limit is approximately a factor 10 to 5 better than the best previously published limit obtained by the Crystal Barrel collaboration [9].

Our result can also be used to constrain the magnitude of the coupling of a hypothetical gauge X boson to quarks [6, 11]

$$g^2 < 2 \times 10^{-7}(1 - \frac{m_X^2}{m_\pi^2})^{-3} \qquad (3)$$

The attenuation of the X- flux due to X interactions with matter was found to be negligible, since for $Br(\pi^0 \to X\gamma) \leq 10^{-4}$ the X boson mean free path in iron is ≥ 300 km, as compared with the iron and earth shielding total length of 0.4 km used in our beam. Furthermore the decay length for $E_X > 10\ GeV$ was estimated to be longer than ≃10 km [11]. We note that limits on the

branching ratio $Br(\eta, \eta' \to \gamma + X)$ could also be obtained from our data if the cross-sections for η, η' productions in the forward direction in $p - Be$ collisions at 450 GeV were known.

Acknowledgements

We thank the SPS staff, the neutrino beam group and the technical staffs of the participating institutions for their vital contributions to the success of this experiment.

This experiment was supported by the Australian Research Council and the Department of Industry, Science and Technology, the Bundesministerium für Bildung, Wissenschaft, Forschung und Technologie of Germany, CERN, the Institut National de Physique Nucléaire et des Particules and the Commissariat à l'Energie Atomique of France, the Istituto Nazionale di Fisica Nucleare of Italy, the Institute for Nuclear Research of the Russian Academy of Sciences and Russian Foundation for Fundamental Research, the Fonds National Suisse de la Recherche Scientifique, the U.S. Department of Energy and the U.S. National Science Foundation, which are gratefully thanked. We are indebted to John Ellis and Nikolai Krasnikov for fruitful discussions.

References

[1] P. Langacker , Phys.Rep. **72C**(1981)185.

[2] S. Weinberg , Phys.Rev.**D26**(1982)287;
P. Fayet, Phys.Lett. **69B**(1977)489, Nucl.Phys. **B187**(1981)184.

[3] J. Ellis et al., Nucl.Phys. **B276**(1986)14.

[4] S. Glashow, Proc. Conf. Rencontres de Moriond, (1986).

[5] M.I. Dobroliubov and A.Yu. Ignatiev, Nucl.Phys. **B309**(1988) 655.

[6] M.I. Dobroliubov, Yad.Fiz. **52**(1990) 551 [Sov.J.Nucl.Phys. **52**(1990) 352].
M.I. Dobroliubov, Z.Phys. **C 49**(1991) 151.

[7] R. Meijer Drees et al., Phys.Rev.**D49**(1994) 4937.

[8] M.S. Atiya et al., Phys.Rev.Lett.**69**(1992) 733.

[9] C. Amsler et al., Phys.Lett. **B333**(1994) 271;
C. Amsler et al., Z.Phys. **C 70**(1996) 219.

[10] R. Meijer Drees et al., Phys.Rev.Lett.**68**(1992) 3845.

[11] S.N. Gninenko and N.V. Krasnikov, "On search for a new light gauge boson from $\pi^0(\eta) \to \gamma + X$ decays in neutrino experiments", hep-ph/9802375, to appear in Phys.Lett.**B**.

[12] J. Altegoer et al. (NOMAD Collaboration), " The NOMAD Experiment at the CERN SPS", Nucl.Instr. and Meth. **A404**(1998)96.

[13] M. Anfreville et al., "The drift chambers of the NOMAD detector", to be submitted to Nucl.Instr. and Meth.(1997).

[14] G. Bassompierre et al., Nucl.Instr. and Meth. **A403**(1998)363.
G. Bassompierre et al., "Performances of the NOMAD Transition Radiation Detector", LAPP-EXP-97-06, to appear in Nucl.Instr. and Meth..

[15] D. Autiero et al., Nucl.Instr. and Meth. **A373**(1996)358.

[16] GEANT: Detector description and simulation tool, CERN Programming Library Long Writeup W5013.

[17] G. Ingelman, The LUND MC for Deep Inelastic Lepton-Nucleon Scattering, LEPTO 6.1, Physics at HERA, October 1991;
T. Sjöstrand, Computer Physics Commun. **39**(1986)347;
H.U.Bengtsson and T.Sjöstrand, JETSET, Computer Physics Commun.**43**(1987)367.

[18] "Parameterization of e^- and γ initiated showers in the NOMAD lead glass calorimeter", to be submitted to Nucl.Instr. and Meth..

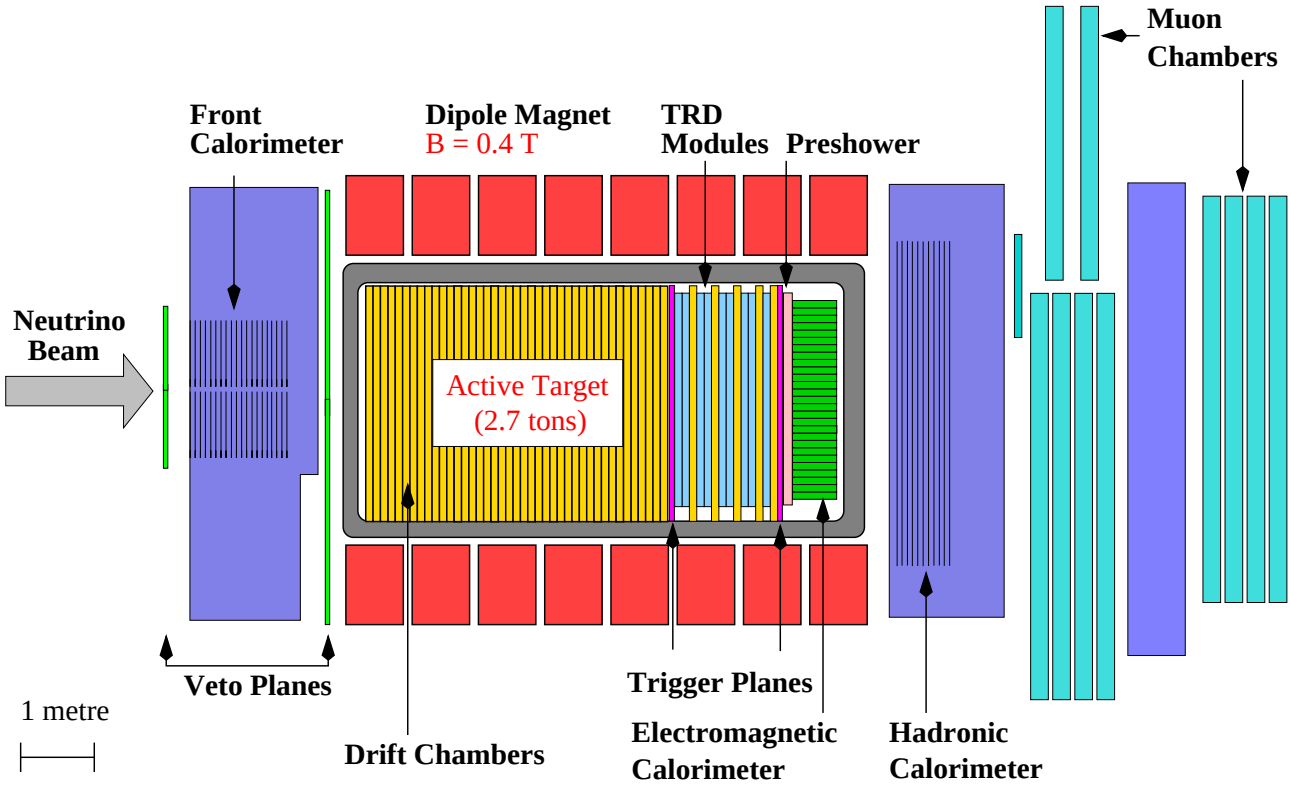

Figure 1: *Side view of the NOMAD detector.*

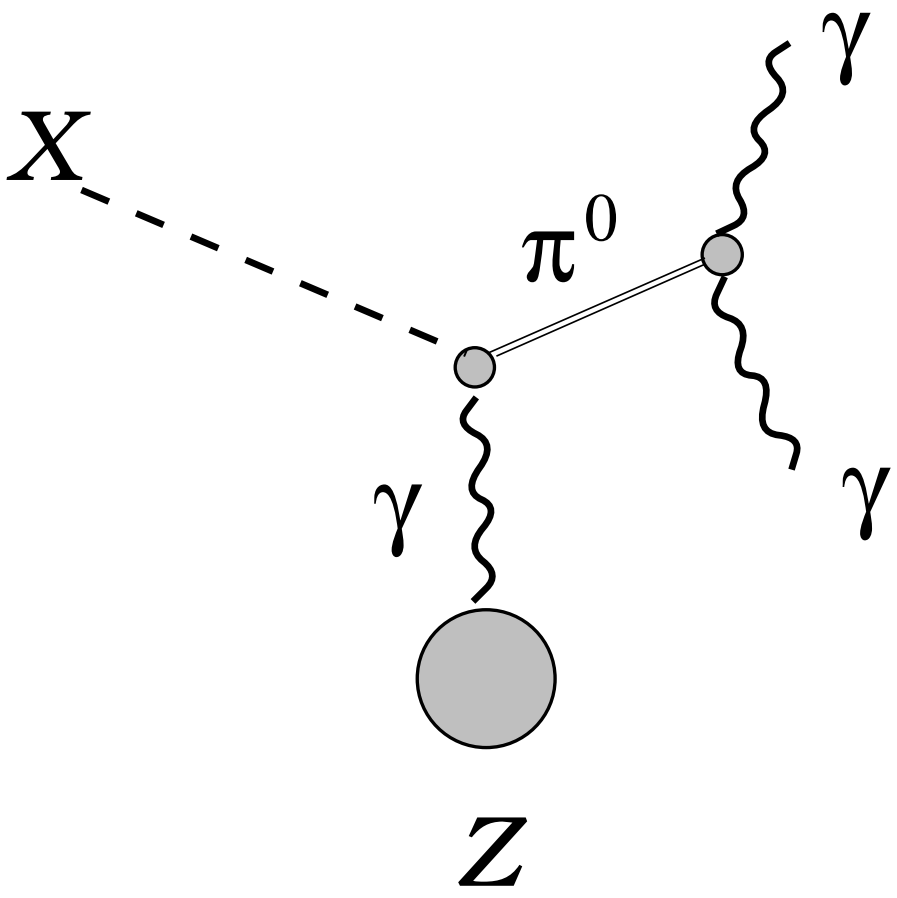

Figure 2: *Feynman diagram for π^0 production by Primakoff effect.*

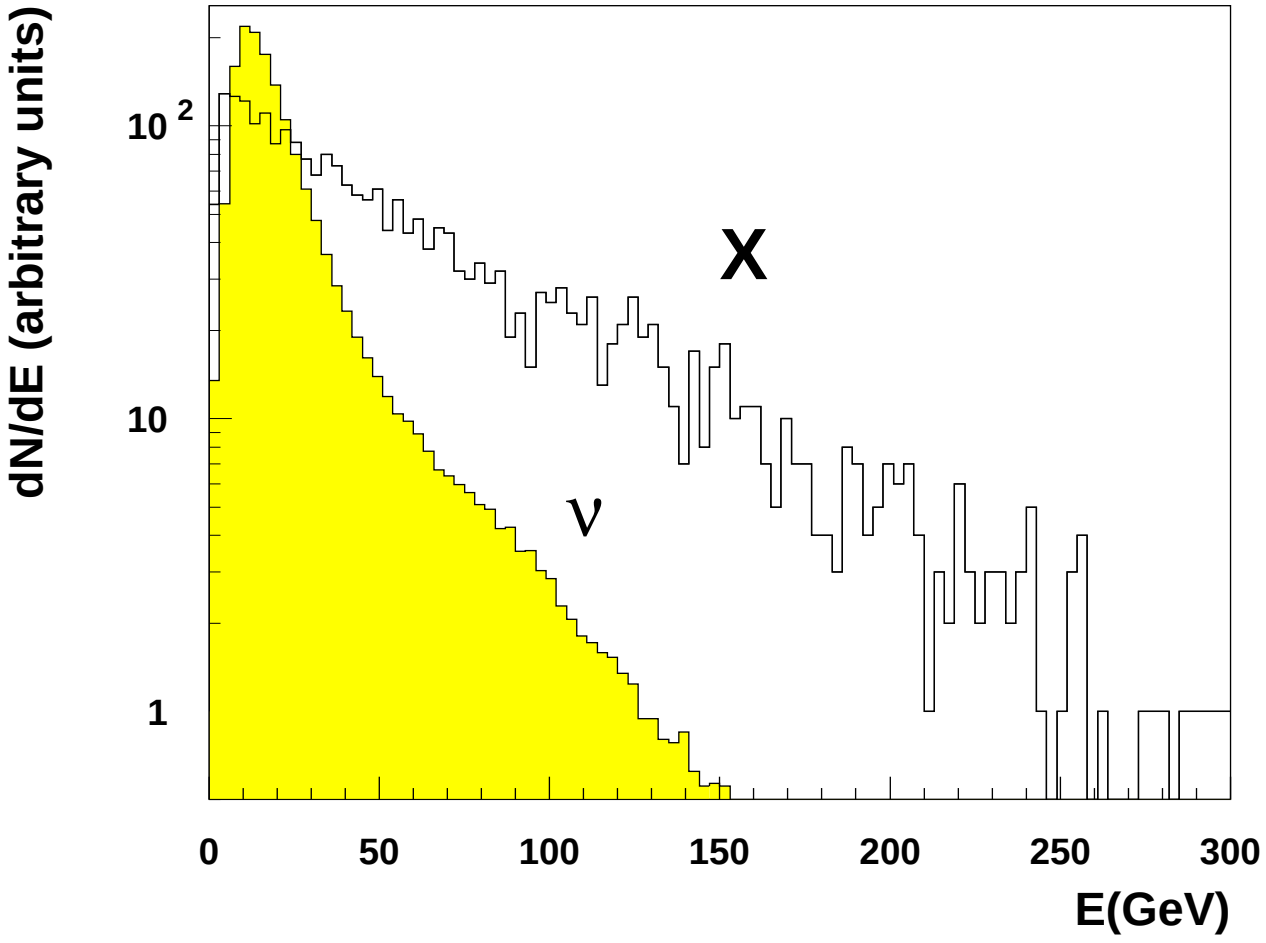

Figure 3: *Combined energy spectrum of X bosons with mass M_X=10 MeV from the SPS neutrino target and from the beam dump region at the NOMAD detector. The neutrino energy spectrum (hatched area) is also shown for comparison. The two spectra are arbitrarily normalized.*

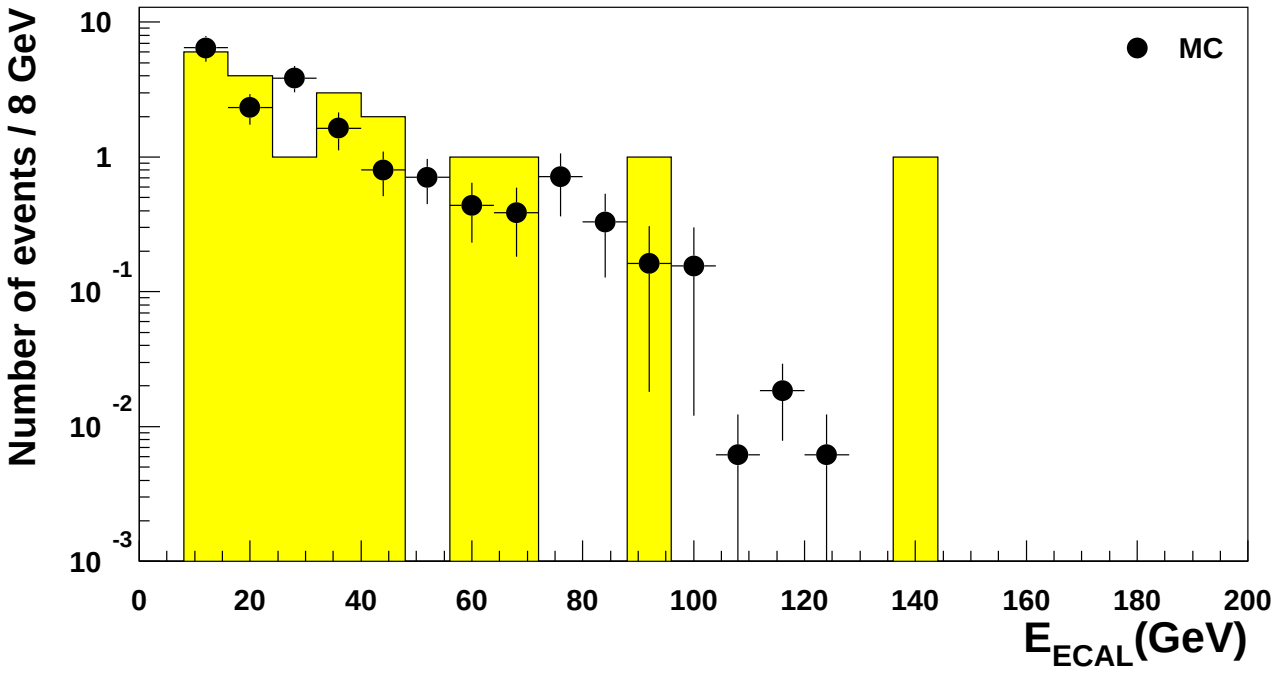

Figure 4: *ECAL energy distributions for candidate events (shaded area) and for combined background events.*

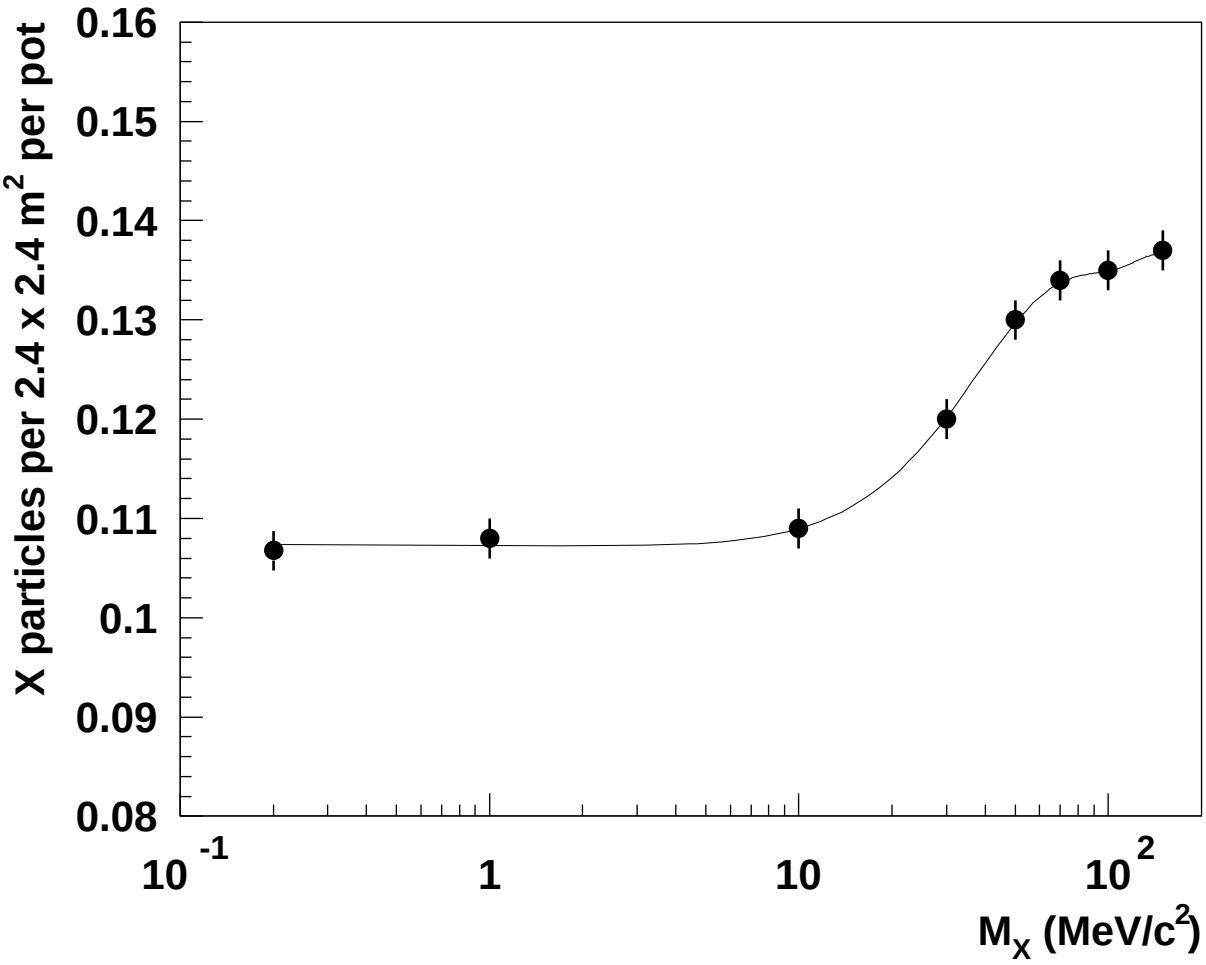

Figure 5: *Total X boson flux at the NOMAD detector versus mass M_X ($E_X > 8$ GeV) calculated for $Br(\pi^0 \to \gamma + X)$=1. The curve is a polynomial fit to the points.*

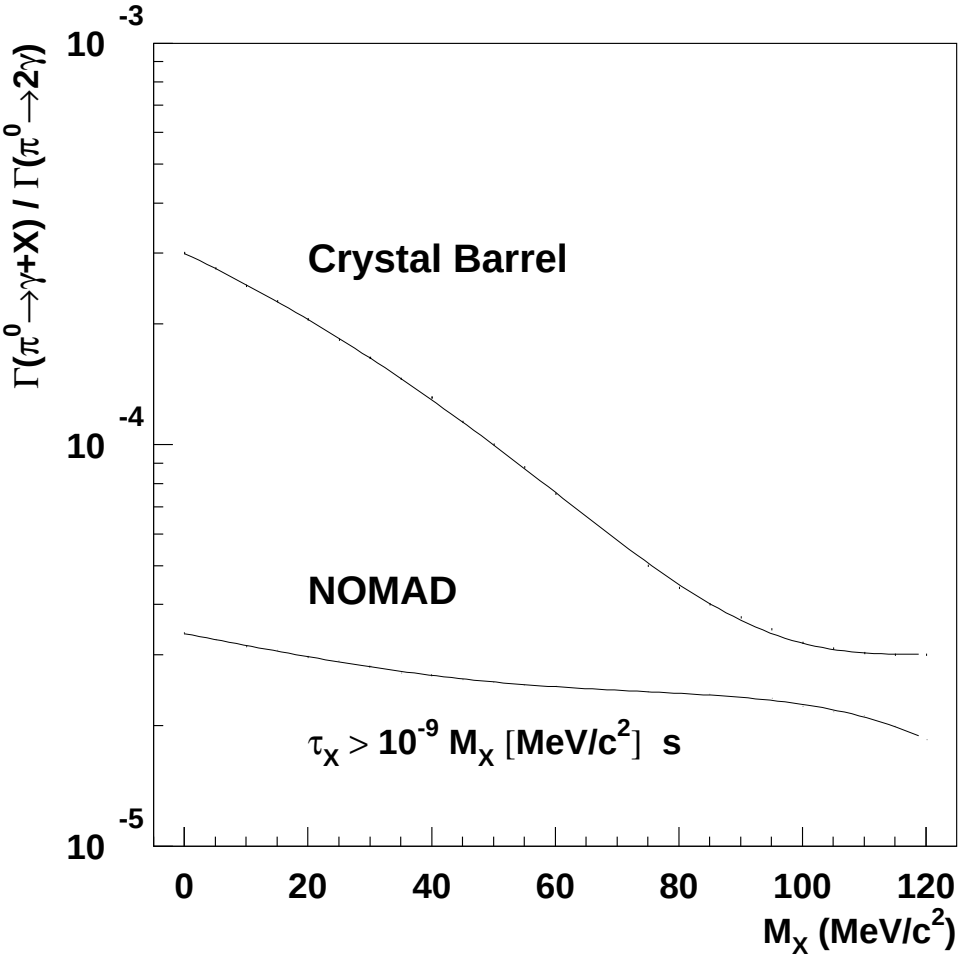

Figure 6: *90% confidence level upper limit on branching* $Br(\pi^0 \to \gamma + X)$ *versus* M_X. *The limit is valid for a lifetime of the* X *boson* $\tau_X > 10^{-9} M_X[MeV/c^2]$ *s.*